Load Frequency Control of Multi-area Hybrid Power System Using Symbiotic Organisms Search Optimized Two Degree of Freedom Controller

More Raju*‡, Lalit Chandra Saikia*, Nidul Sinha*

*Department of Electrical Engineering, National Institute of Technology Silchar, Silchar, Cachar, Assam, India, 788010

(more.raju.in@ieee.org, lcsaikia@yahoo.com, nidulsinha@hotmail.com)

‡Corresponding Author; More Raju, Tel: +91 9533817703,

more.raju.in@ieee.org

Received:21.03.2017 Accepted:26.04.2017

Abstract- This paper presents the load frequency control of three area interconnected system. Area1 comprises of thermal and distributed generation (DG) resources. Area2 and area3 are having thermal generations. The DG combination with conventional thermal generation makes the system hybrid. The DG resources comprises of wind turbine generator, diesel engine generator, fuel cell, aqua-electrolyzer and battery energy storage system. The single degree of freedom integral (I), proportional integral (PI), proportional integral derivative (PID) and two-degree of freedom-PID (2-DOF-PID) controllers are applied as secondary controllers in the system. These controller's gains and additional parameters are simultaneously optimized with new powerful and robust metaheuristic technique named symbiotic organisms search (SOS) technique. Studies disclose the superior performance of 2-DOF-PID over other controllers in providing the reduced peak overshoots, minimum settling time and lesser value of cost function. Comparative performances of various algorithms prove superiority of SOS over others. Sensitivity analysis exposes the toughness of optimum gains and additional parameters of 2-DOF-PID controller attained for nominal conditions to large alteration in system loading condition, inertia parameter and magnitude, location of perturbation. The 2-DOF-PID controller also performs satisfactorily for random load perturbation and random wind generator input.

Keywords Distributed generation resources, load frequency control, symbiotic organisms search, two degree of freedom controller, wind generator.

1. Introduction

In an interconnected power system, the mismatch between the generation and demand creates the deviations in the frequency and tie line powers from their nominal values. These deviations must be maintained in the proper limits to achieve the efficient, economic and reliable operation, failing which may cause the undesirable situations like power system collapse. Load frequency control (LFC) maintains the continuous monitoring between demand and generation by adjusting the output of the generator in accordance with load requirement [1].

The load demand is increasing day by day due to various reasons such as rapid growth in population and modernization. The constant use of conventional sources for power generation leads to a stage that these sources are depleted in a very short time. Moreover, the cost of fuel is also increasing time to time. Owing to this non-conventional energy from wind, photo voltaic, bio-fuels etc., in the form of the distributed generation (DG) resources attracted the attention of researchers [2-8]. However, DG resources are having less generation capacity as compared to conventional generations. As DG resources are placed near to the consumers, the transmission losses are also less. The DG resources with wind generation makes the power system control more complicated. The frequency response for wind farms is enhanced by using hybrid energy storage system in [9]. Hui et al. [10] presented the LFC issues with diffusion of

wind generation. The studies on system with DG resources consisting of wind turbine generator (WTG), diesel engine generator (DEG), aqua electrolyzer (AE), fuel cell (FC) and energy storage units are available in [11]. Similarly, authors in [12] presented studies with integration of various sources like off shore wind, photovoltaic (PV), FC, DEG and energy storage system.

Literature survey reveals that significant amount of work has done in the field of LFC [13-15]. Sahu et al. [13], Pathak et al. [14] and Gozde et al. [15] studied LFC of interconnected two-area thermal system. Elsisi et al. [16] presented LFC of two-area interconnected hydro-thermal system. Raju et al. [17] carried out studies on unequal three area thermal system. Authors in [18] presented LFC studies in two area and three area systems. Saikia et al. [19, 20] presented LFC studies on three area hydro-thermal system.

Pandey et al. [21] presented LFC of hybrid power system, in which DG resources are linked with existing power system. However, studies in [21] are restricted to isolate and two-area systems only. Moreover, the realistic parameter generation rate constraints (GRC) is not considered in their study. The three area LFC comprising of DG resources is not presented in any study till date. This promotes for future study.

The governor of the generating unit has two controls. The speedy primary control and the sluggish secondary control. Recent research in LFC is mainly centered on the design of secondary controller (SC). Nanda et al. [22] utilized classical integral (I) and proportional integral (PI) controllers as SC. Authors in [23, 24] applied proportional integral derivative (PID) controller as SC in LFC studies. Saikia et al. [25] studied the comparative performance of several one-degree of freedom (1-DOF) classical controllers namely I, PI, PID, ID and I double D (IDD) controllers. Investigations in [25] reveal the better performance of IDD controller over ID, PID, PI and I controllers. Sahu et al. [13] have presented the two-DOF-PID (2-DOF-PID) controller as SC in LFC study. Studies in [26, 27] are presented with 2-DOF-PID as SC. Dash et al. [28] presented comparative performances of 2-DOF controllers in LFC. The 2-DOF controllers have the advantages of achieving the high performance for set-point tracking as well as regulation in the incidence of perturbated inputs as compared to 1-DOF controllers. However, the 2-DOF-PID controller is not investigated as SC in any LFC study with consideration of DG resources. This needs further study.

Critical literature survey reveals that efforts have been done to propose different control methodologies. Optimal [29], fuzzy [19], neural [20] control strategies applied successfully to solve LFC problem. The LFC problem, not only deals with the selection of the secondary controller (SC) but also its designing i.e. SC gains and additional parameters should be selected properly in order to force the area control error i.e. ACE to zero. The expression ACE represents the combined deviations of frequency and tie-line powers. Numerous optimization techniques like genetic algorithm (GA) [30], non-dominated sorting GA-II (NSGA-II) [23], craziness based particle swarm optimization (CPSO) [15], artificial bee colony (ABC) [31], differential evolution (DE) [13, 18], bacterial foraging optimization (BFO) [19, 24], cuckoo search (CS) technique [28], firefly algorithm (FA) [32], bat algorithm (BA) [16], antlion optimization (ALO) [17] techniques etc., are successfully applied in conventional LFC to optimize different SC gains and their different parameters. Saikia et al. [19] presented better performance of BFO technique over GA and PSO techniques in terms of the convergence characteristics. The differential evolution (DE) technique performed better than CPSO in [13] and GA, PSO, FA techniques in LFC [18]. Elsisi et al. [16] applied BA that performed better than GA. The NSGA-II performed well over BFO, GA and PSO techniques [23]. Authors in [26] showed the superiority of teaching learning based optimization algorithm (TLBOA) over conventional Ziegler Nichols (ZN), GA, BFOA, DE and hybrid BFOA-PSO techniques. Studies in [32] explore the better performance of FA technique over BFO algorithm.

Recently, a new powerful and robust metaheuristic technique named symbiotic organisms search (SOS) [33] attains the focus of researchers. It is successfully applied to test 26 mathematical problems (unconstrained) and 4 structural design engineering problems. The SOS technique simulates the interaction of organisms for surviving and propagation in the ecosystem. Biological interactions among various organisms in ecosystem are represented through different phases namely mutualism, commensalism and parasitism phases. The main benefit of SOS optimization technique over other techniques is that it requires no particular algorithm parameter, although its characteristics are equivalent to most of the population based techniques. However, the SOS algorithm is yet to be studied to optimize the various gains and different parameters of SCs in LFC of hybrid system.

Authors in [17, 20, 25, 28, 32, 34] presented the sensitivity analysis (SA) to examine the toughness of nominal controller gains and different parameters of SC found at nominal system conditions for large alterations in the nominal system loading condition, inertia constant (H), magnitude and location of perturbation. However, the sensitivity analysis is not performed for unequal three area LFC consisting of DG resources. This motivates the authors.

Raju et al. [17] and Dash et al. [34] studied the performance of PID plus double D controller [17] and cascade 1-DOF-PD and 1-DOF-PID [34] against random load pattern (RLP) as perturbation. However, SOS optimized 2-DOF-PID controller performance is not presented in any LFC study against RLP. This needs to be studied.

Summarizing the above discussion, the main contributions of current work are:

a) To develop an interconnected unequal three area power system comprising of DG resources and thermal generation in area1 and thermal generation in area2 and area3 with consideration of appropriate GRC.
b) To apply 2-DOF-PID, PID, PI and I controllers as SCs and optimization of these SCs gains and different parameters with SOS technique and to compare the dynamic behaviors to find the best.
c) To perform the sensitivity analysis for the superior controller (found in b)) gains and different parameters achieved at nominal system conditions for varied system loading conditions, inertia

parameter (H) and different SLP (magnitude, location) conditions.

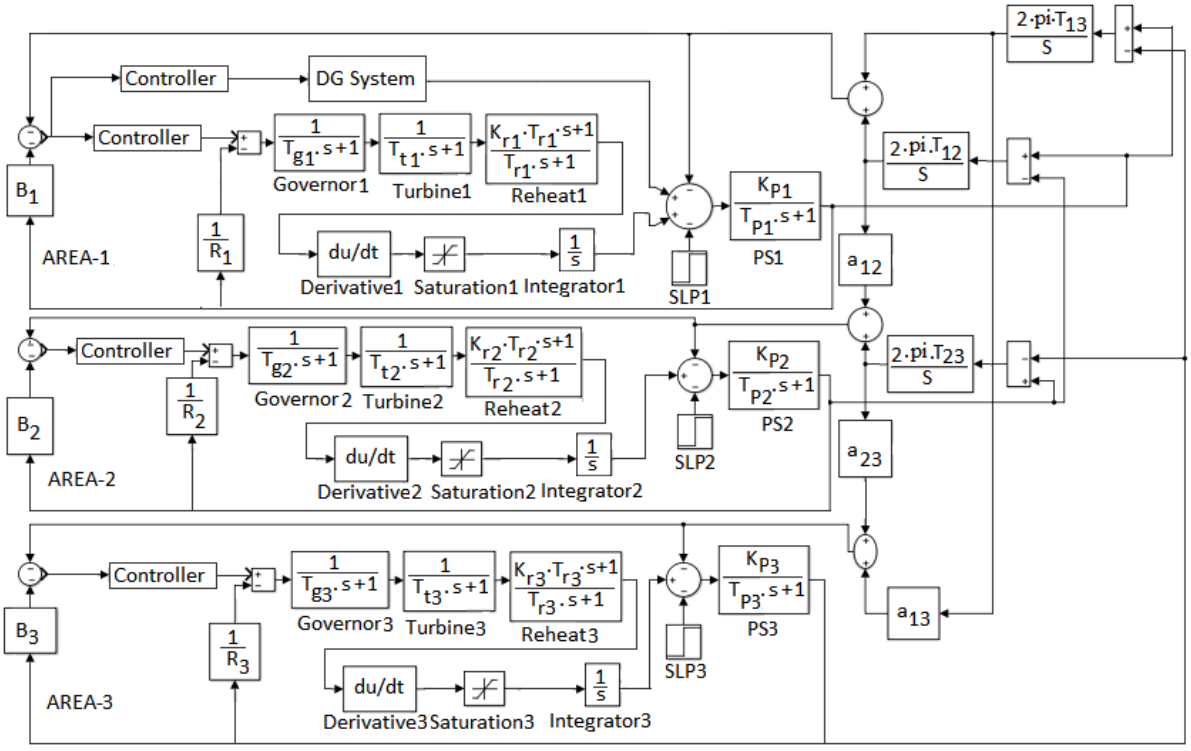

Fig. 1. The mathematical model of hybrid system with secondary controller.

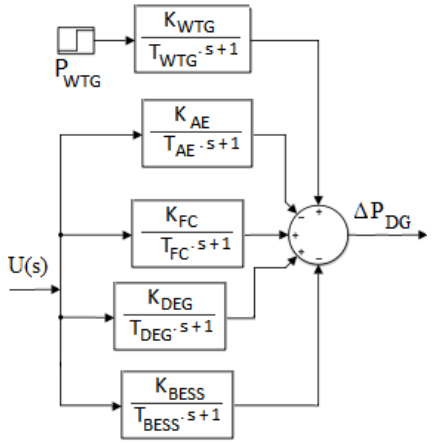

Fig. 2. Mathematical model of the distributed generation (DG) resources.

d) To analyze the effectiveness of better controller found in b) when, (i) the nature of perturbation changed to RLP from SLP, (ii) random wind generator input is applied.

2. System Studied

A three area system is considered with capacity ratio of area-1: area-2: area-3 as 1: 4: 6. In area-1, in addition to thermal generation, distributed generation (DG) resources are considered that makes the system hybrid. The distributed generation (DG) resources considered here are the combination of wind turbine generator (WTG), aqua electrolyzer (AE), fuel cell (FC), diesel engine generator (DEG) and battery energy source system (BESS). The area-2 and area-3 consist of thermal generations. The thermal generations are provided the generation rate constraints (GRC) of 3% per minute. The nominal system parameters are adopted from [12, 17, 35] and are shown in Appendix. Several controllers, namely 2-DOF-PID, PID, PI, and I are applied as secondary controllers (SCs). The study system transfer function model is represented in Fig.1. In Fig.2, the transfer function model of distributed generation (DG) resources system is shown. Matlab/Simulink software package used for coding of SOS and development of the system model.

The various SCs gains and different parameters are optimized with metaheuristic technique named symbiotic organisms search (SOS) algorithm subjected to minimize cost function (*J*) using integral squared error (ISE) criterion (Eq. (1)).

$$J = \int_0^T \left(\Delta f_i^2 + \Delta P_{tiei-h}^2\right) dt \quad (1)$$

where, i, h = area number (i, h = 1, 2, 3; i ≠ h) and T is the simulation time (s).

3. Two-Degree of Freedom (2-DOF) Controller

The closed loop transfer functions that are adjusted independently for a system is termed as degree of freedom (DOF). Generally, the design of the control system is multi objective function, hence two-DOF (2-DOF) structures always provides the advantage over one-DOF (1-DOF) control structure [36]. The 2-DOF structure is applied successfully in the field of control engineering owing to its enhanced control quality meant for not only fine set-point variable tracking but also for better disturbance rejection [37, 38]. There are two inputs for 2-DOF controller, namely reference signal and measured output signal. The 2-DOF scheme yields the output signal depends on difference of a

reference signal (R(s)) and calculated system output (Y(s)). The 2-DOF structure has proportional set-point weightings (b_i) and derivative set-point weightings (c_i). Based on the set-point weightings, a weighted modified signal for derivative, integral and proportional actions is calculated. Each specified action is weighted in accordance to the selected gain limits. The Fig.3 shows the 2-DOF control scheme, in which R(s) denotes the reference signal, Y(s) denotes feedback from measured system output, C(s) is 1-DOF controller and F(s) is the pre-filter on R(s). The U(s) represents output signal. For a 2-DOF-PID controller, F(s) and C(s) are given by Eq. (2) and Eq. (3).

$$F(s) = \frac{(bK_{Pi} + cK_{Di}N_i)s^2 + (bK_{Pi}N_i + K_{Ii})s + K_{Ii}N_i}{(K_{Pi} + K_{Di}N_i)s^2 + (K_{Pi}N_i + K_{Ii})s + K_{Ii}N} \quad (2)$$

$$C(s) = \frac{(K_{Pi} + K_{Di}N_i)s^2 + (K_{Pi}N_i + K_{Ii})s + K_{Ii}N_i}{s(s + N_i)} \quad (3)$$

where, K_{Di}, K_{Ii}, and K_{Pi} are the derivative, integral and proportional gains respectively, b_i and c_i are the set-point weights of proportional and derivative actions respectively, and N_i is the filter coefficient for derivative action. The proposed 2-DOF-PID controller structure is presented in Fig.4.

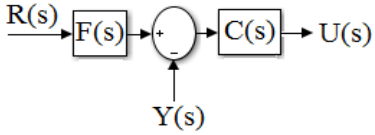

Fig. 3. The two-degree of freedom (2-DOF) control scheme.

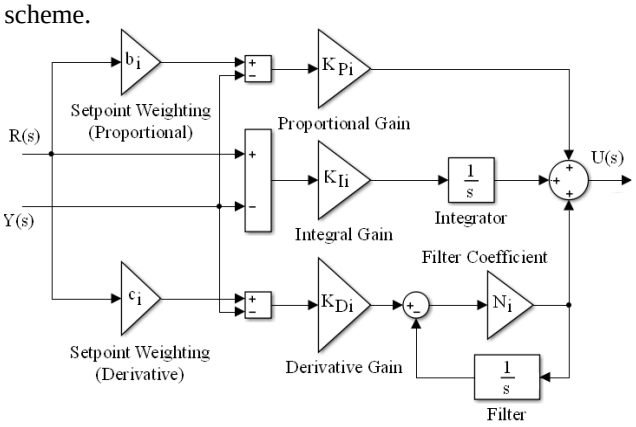

Fig. 4. The transfer function of 2-DOF-PID controller.

4. Symbiotic Organisms Search (SOS) Technique

Symbiotic organisms search (SOS) technique, is a latest, robust and powerful metaheuristic technique proposed by Cheng and Prayogo [33]. It simulates the symbiotic interaction among organisms for surviving in the ecosystem and does not require any specific algorithm parameter. Symbiosis is originated from Greek word that means "living together". In SOS, the population space is called as ecosystem and new solutions can be generated by biological interaction among organisms in ecosystem. The SOS technique uses three phases which resembles real biological interaction namely mutualism, commensalism and parasitism phases. Flowchart for the SOS technique is shown in Fig.5.

4.1. The Mutualism Phase

In this phase, both the organisms in interaction will get the benefit like the relationship between bees and flowers. Bees collect nectar to turn into honey from flowers and flowers also benefit by bees which distribute the pollen. Let X_k is selected randomly to interact with X_j organism of eco-system both will continue the relation to increase the mutual survival in eco-system. New values for X_j and X_k by mutualism phase is given by Eq. (4) and Eq. (5).

$$X_{jnew} = X_j + rand(0,1).(X_{best} - MV.BF_1) \quad (4)$$

$$X_{knew} = X_k + rand(0,1).(X_{best} - MV.BF_2) \quad (5)$$

where, $MV = Mutual\_Vector = \frac{X_j + X_k}{2}$, rand(0, 1) is the vector of random numbers and BF_1 and BF_2 are called as the benefit factors. Generally BF_1 and BF_2 are taken either 1 or 2 which denote the level of advantage to each organism. The *MV* (mutual vector) represents the relationship characteristic between X_j and X_k .

4.2. The Commensalism Phase

In this phase, benefit for one organism while other organism will not get any impact like relation between sharks and remora fish. The remora fish gets benefit by attaching itself to the sharks and eats food leftover, while shark unaffected by this activity. Let X_k selected randomly to interact with X_j from the ecosystem such that X_j gets benefit with the interaction while X_k neither suffers nor benefits. Hence, X_j can be updated using Eq. (6).

$$X_{jnew} = X_j + rand(-1,1).(X_{best} - X_k) \quad (6)$$

X_j will be updated only when the new fitness is improved than the pre-interaction fitness. The (X_{best} –X_k) is the benefit provided by X_k to X_j to increase its survival advantage in ecosystem.

4.3. The Parasitism Phase

In this phase, one organism gets benefit from the other while other organism is affected harmly like the relationship between anopheles mosquito (parasite) and human body. Anopheles mosquito thrives and reproduces within the human body, while human host may suffer from malaria. Let X_j is given the role of mosquito by creating parasite vector, which is formed by duplicating organism X_j. Let X_k selected randomly which is given the role of host. If parasite vector fitness is greater than X_k, it kills X_k and adopts its position. If X_k fitness is more than parasite vector, then X_k will have more immune and parasite vector will no more exists in the ecosystem.

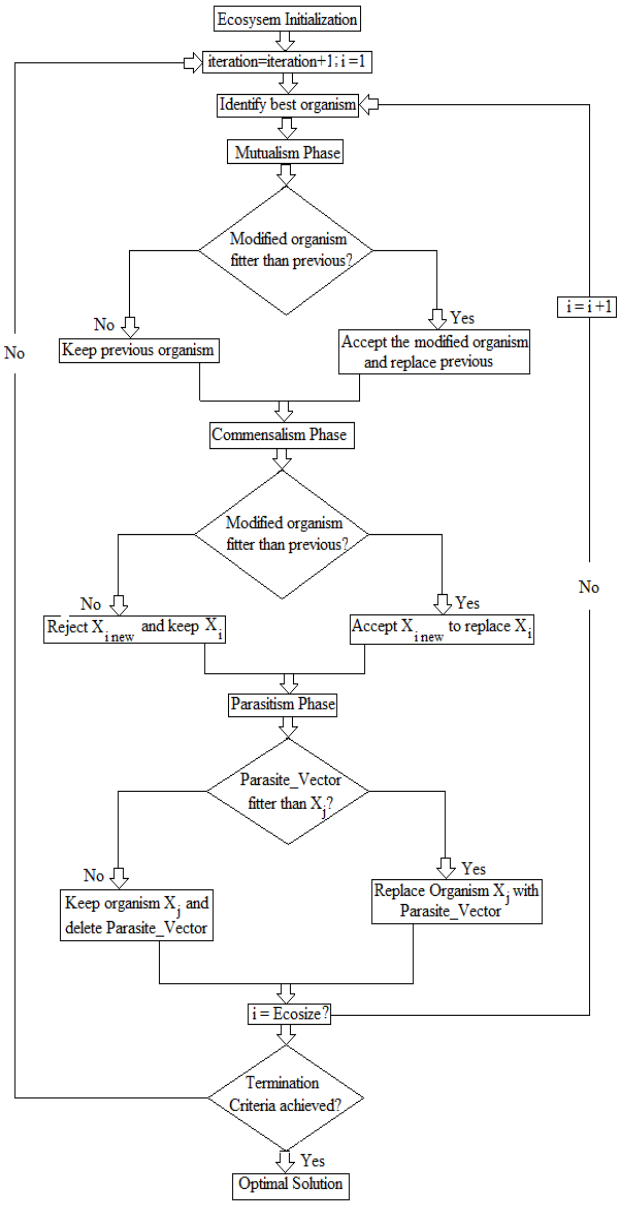

Fig. 5. Flowchart of symbiotic organisms (SOS) technique.

The ecosize (n) = 100, function evaluations (FE) = 5000, the benefit factors (BF_1, BF_2) are chosen randomly either 1 or 2. The gains and other parameters of 2-DOF-PID, PID, PI and I are optimized using SOS technique subjected to minimum of *J*.

5. Results and Analysis

5.1. Optimization of gains and additional parameters of 1-DOF-I, 1-DOF-PI, 1-DOF-PID and 2-DOF-PID controllers

The single degree of freedom (1-DOF) PID, PI, I and two-degree of freedom-PID (2-DOF-PID) controllers considered separately as secondary controllers (SCs) for the proposed system. In each case, the SCs gains and different parameters (in case of PID and 2-DOF-PID) are optimized concurrently using SOS technique with consideration of 1% SLP in area1 and P_{WTG} as 1% rated capacity of area1. The attained optimum values are given in Table 1. The dynamic responses with these optimum parameters (Table 1) for various secondary controllers (2-DOF-PID, PID, PI and I) are plotted and compared in Fig.6. The settling time (STs) and peak overshoots (POs) of these responses are given in Table 2.

Table 1. The optimum values of 2-DOF-PID, PID, PI and I controller at nominal system conditions.

Controller	Optimum values
I	K_{IDG}^* = 0.3352; K_{I1}^* = 0.5252; K_{I2}^* = 0.5252; K_{I3}^* = 0.5210.
PI	K_{IDG}^* = 0.1120; K_{I1}^* = 0.1230; K_{I2}^* = 0.2230; K_{I3}^* = 0.2141; K_{PDG}^* = 0.1020; K_{P1}^* = 0.0301; K_{P2}^* = 0.1020; K_{P3}^* = 0.0820.
PID	K_{IDG}^* = 0.5241; K_{I1}^* = 0.5241; K_{I2}^* = 0.3252; K_{I3}^* = 0.0525; K_{PDG}^* = 0.1254; K_{P1}^* = 0.1241; K_{P2}^* = 0.3252; K_{P3}^* = 0.0525; K_{DDG}^* = 0.1001; K_{D1}^* = 0.0852; K_{D2}^* = 0.0525; K_{D3}^* = 0.0525; N_{DG}^* = 78.3651; N_1^* = 56.3252; N_2^* = 85.6321; N_3^* = 65.3201.
2-DOF-PID	K_{IDG}^* = 0.0050; K_{I1}^*= 0.0960; K_{I2}^* = 0.1516; K_{I3}^* = 0.5198; K_{PDG}^* = 1.0000; K_{P1}^* = 0.0493; K_{P2}^* = 1.0000; K_{P3}^* = 0.9976; K_{DDG}^* = 0.9978; K_{D1}^* = 0.2248; K_{D2}^* = 0.3041; K_{D3}^* = 0.8798; N_{DG}^* = 10.0000; N_1^* = 56.3252; N_2^* = 37.6263; N_3^* = 82.0506; b_{DG}^* = 0.9586; b_1^* = 0.5095; b_2^* = 0.9539; b_3^* = 0.9082; c_{DG}^* = 1.0000; c_1^* = 0.2116; c_2^* = 0.9525; c_3^* = 0.2545.

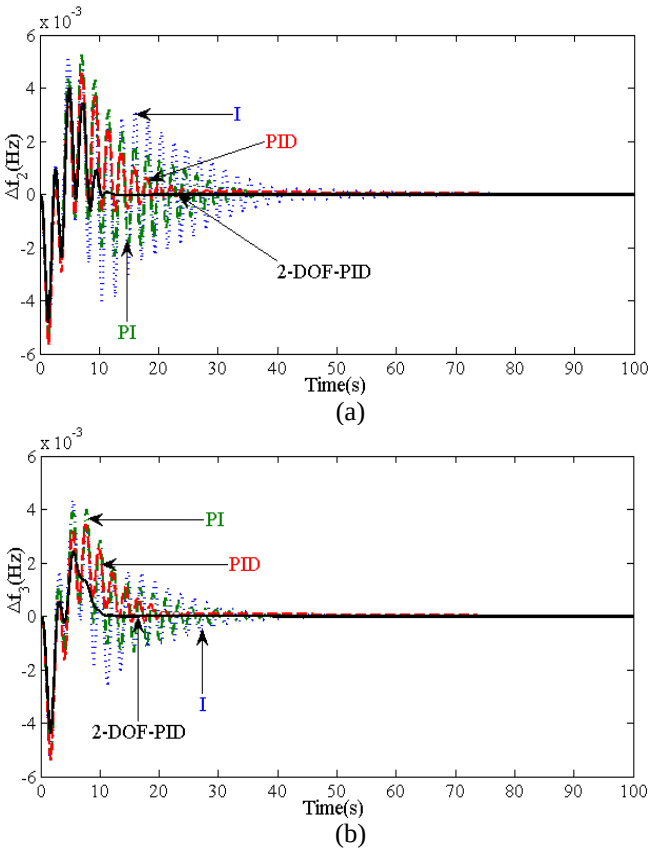

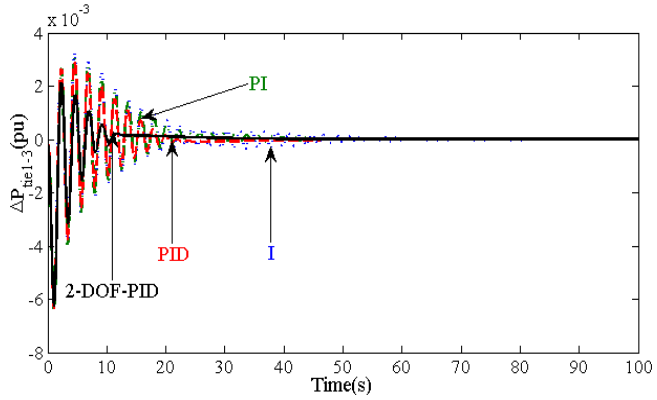

(c)

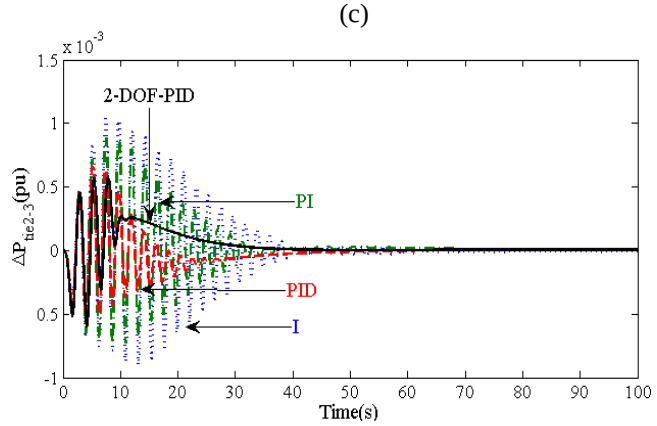

(d)

Fig. 6. The comparative dynamics for 2-DOF-PID, PID, PI and I controllers.
(a) Δf_2 vs. Time (s).
(b) Δf_3 vs. Time (s).
(c) ΔP_{tie1-3} vs. Time (s).
(d) ΔP_{tie2-3} vs. Time (s).

Table 2. Comparison of STs and POs for Fig.6.

Response	Settling time, ST (s)				Peak overshoots (PO) (X 10^{-3})			
	I	PI	PID	2-DOF-PID	I	PI	PID	2-DOF-PID
Δf_2	77	52	46	20	5	5	4	3
Δf_3	51	44	37	12	4	4	3	2
ΔP_{tie1-3}	79	47	37	30	3	3	2.8	2.1
ΔP_{tie2-3}	86	71	57	45	1	0.8	0.6	0.57

From Fig.6 and Table 2, it is clear that peak overshoots, settling time (s) and magnitudes of oscillations corresponding to 2-DOF-PID controller are lesser than that of PID, PI, and I controllers. The cost (*J*) value for 2-DOF-PID, PID, PI and I controllers are 0.00081, 0.00140, 0.00165 and 0.00191 respectively. This proves the superiority of 2-DOF-PID over others.

To test the performance of SOS technique, the other set of techniques such as particle swarm optimization (PSO) and firefly algorithms (FA) are utilized for optimizing the gains and different parameters of 2-DOF-PID controller for the same system considered in Fig.1. The gains and different parameters of 2-DOF-PID controller when optimized with PSO and FA techniques are shown in Table 3. With these optimum (Table 3) values, the dynamic responses for PSO, FA and SOS (optimum values of Table 1) are compared in Fig.7. The value of cost function (*J*) obtained with PSO technique is 0.00121 and that of FA technique is 0.00109. From Fig.7 and cost function values, it is observed that SOS technique outperforms PSO and FA techniques in terms of not only improved dynamics but also the cost function (*J*) value.

Table 3. The PSO and FA optimized 2-DOF-PID controller optimum gains and parameters.

Technique	Optimum parameters of 2-DOF-PID controller.
PSO	K_{IDG}^* = 0.2110; K_{I1}^* = 0.0202; K_{I2}^* = 0.0963; K_{I3}^* = 0.0652; K_{PDG}^* = 0.0120; K_{P1}^* = 0.0120; K_{P2}^* = 0.0120; K_{P3}^* = 0.2020; K_{DDG}^* = 0.1202; K_{D1}^* = 0.0096; K_{D2}^* = 0.0200; K_{D3}^* = 0.0202; N_{DG}^* = 81.6464; N_1^* = 88.5680; N_2^* = 92.8463; N_3^* = 93.3251; b_{DG}^* = 0.1200; b_1^* = 0.0210; b_2^* = 0.0933; b_3^* = 0.2425; c_{DG}^* = 0.0963; c_1^* = 0.1200; c_2^* = 0.1200; c_3^* = 0.2574.
FA	K_{IDG}^* = 0.3220; K_{I1}^* = 0.0214; K_{I2}^* = 0.0122; K_{I3}^* = 0.2122; K_{PDG}^* = 0.0211; K_{P1}^* = 0.0552; K_{P2}^* = 0.0122; K_{P3}^* = 0.0525; K_{DDG}^* = 0.9660; K_{D1}^* = 0.0222; K_{D2}^* = 0.08211; K_{D3}^* = 0.1066; N_{DG}^* = 94.9095; N_1^* = 89.2418; N_2^* = 30.8576; N_3^* = 64.9537; b_{DG}^* = 0.2415; b_1^* = 0.2141; b_2^* = 0.3200; b_3^* = 0.2850; c_{DG}^* = 0.6325; c_1^* = 0.7230; c_2^* = 0.2210; c_3^* = 0.5263.

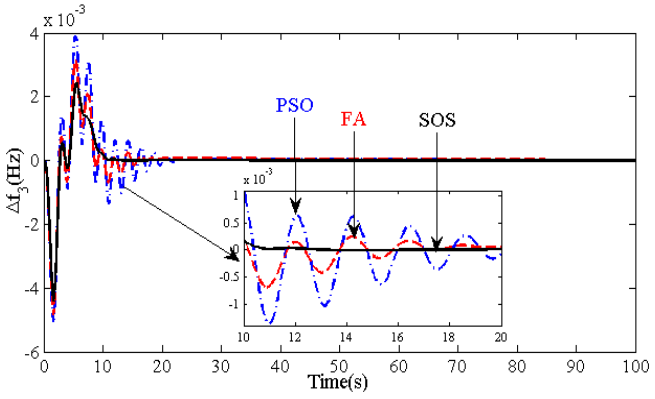

(a)

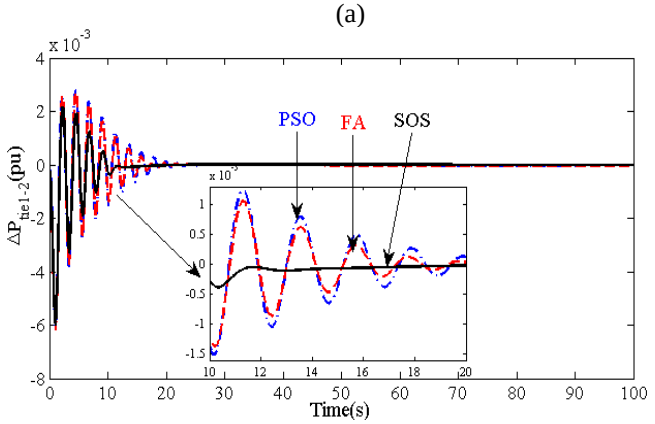

(b)

Fig. 7. The dynamic responses comparison for PSO, FA and SOS techniques.
(a) Δf_3 vs. Time (s), (b) ΔP_{tie1-2} vs. Time (s).

5.2. Sensitivity Analysis

The sensitivity analysis (SA) is performed to check the toughness of proposed 2-DOF-PID controller gains (K_{Ii}^*, K_{Pi}^*, K_{Di}^*) and other parameters (b_i^*, c_i^* and N_i^*) found at nominal circumstances to wide variation in the system circumstances such as system loading condition, system inertia parameter and magnitude, location of step load perturbation.

5.2.1. The SA for varied loading condition

The nominal loading of the system is 50%. It is varied by ±25% i.e. to 25% and 75% loading. At 25% and 75% loading, the 2-DOF-PID controller gains (K_{Ii}, K_{Pi}, K_{Di}) and other parameters (b_i, c_i and N_i) are optimized again using SOS technique and are mentioned in Table 4 (column 2 and column 3). At 25% and 75% loading, the responses are plotted for optimum values at nominal and varied system loading conditions in Fig.8 and Fig.9. It is appreciated from Fig.8 and Fig.9 that the responses (with optimum values for varied and nominal loading) are nearly similar. This confirms the toughness of nominal 2-DOF-PID controller gains and additional parameters for far variation in system loading.

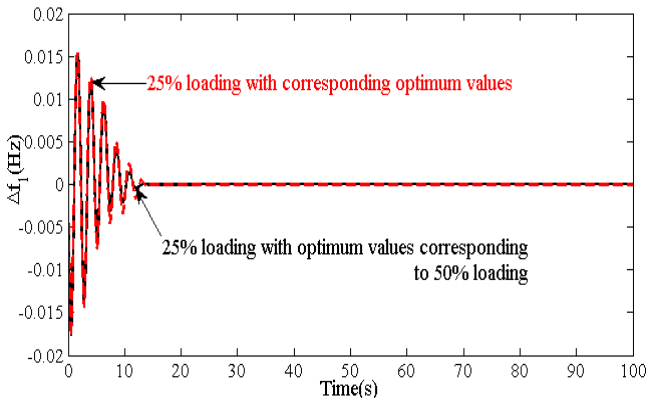

Fig. 8. Δf_1 vs. Time (s) at 25% loading.

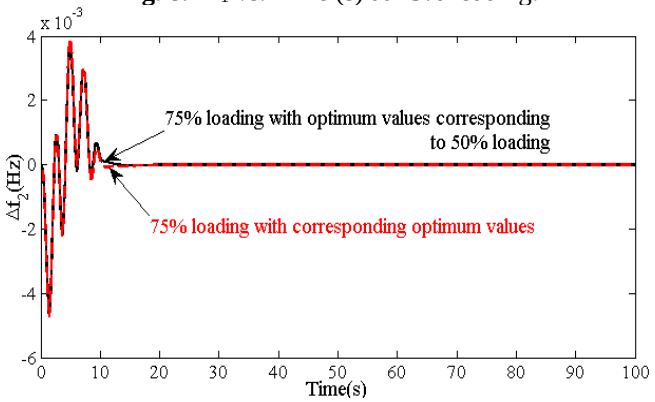

Fig. 9. Δf_2 vs. Time (s) at 75% loading.

5.2.2. The SA for varied inertia constant

The nominal value of system parameter, inertia constant (H) is 5 s. It is varied by ±20% i.e. to 4 s and 6 s. For each varied condition the 2-DOF-PID controller gains (K_{Ii}, K_{Pi}, K_{Di}) and other parameters (b_i, c_i and N_i) are optimized separately using SOS technique and are mentioned in Table 4 (column 4 and column 5). At H = 4 s and H = 6 s, the dynamic responses are plotted with optimum values at nominal and varied system inertia constant (H) in Fig.10 and Fig.11. It is seen from Fig.10 and Fig.11 that the responses (with optimum parameters at varied and nominal H) are almost similar. This confirms the robustness of 2-DOF-PID controller gains and other parameters for variations in system inertia constant.

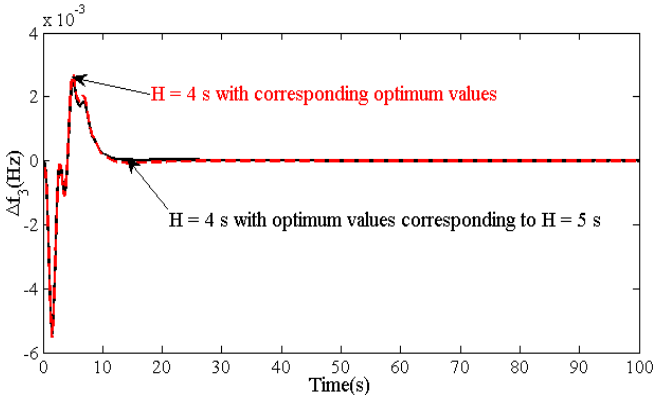

Fig. 10. Δf_3 vs. Time (s) at H = 4 s.

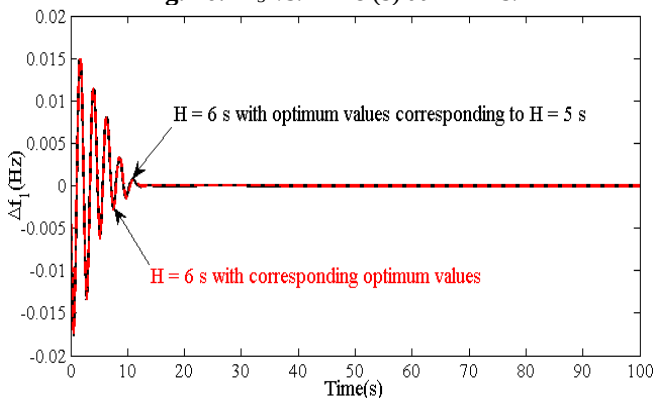

Fig. 11. Δf_1 vs. Time (s) at H = 6 s.

5.2.3. The SA at varied magnitudes of perturbation

The nominal magnitude of perturbation is 1% SLP in area-1. It is incremented by 1% and 2% i.e. to 2% and 3% SLP in area-1. In each varied SLP case, the 2-DOF-PID controller gains (K_{Ii}, K_{Pi}, K_{Di}) and other parameters (b_i, c_i and N_i) are optimized separately using SOS technique and are mentioned in Table 4 (column 6 and column 7). At 2% and 3% SLP in area1, dynamic responses are plotted with optimum values at nominal SLP and varied SLP conditions in Fig.12 and Fig.13. It is observed from Fig.12 and Fig.13 that the responses (with optimum values at varied and nominal SLP conditions) are almost same. This confirms the toughness of 2-DOF-PID controller gains and different parameters for variations in magnitude of perturbation.

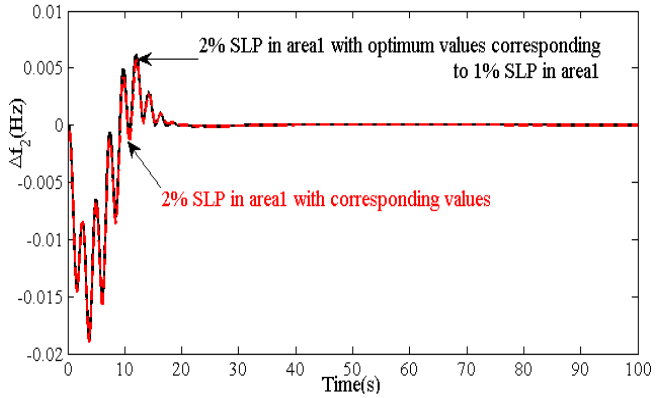

Fig. 12. Δf_2 vs. Time (s) at 2% SLP.

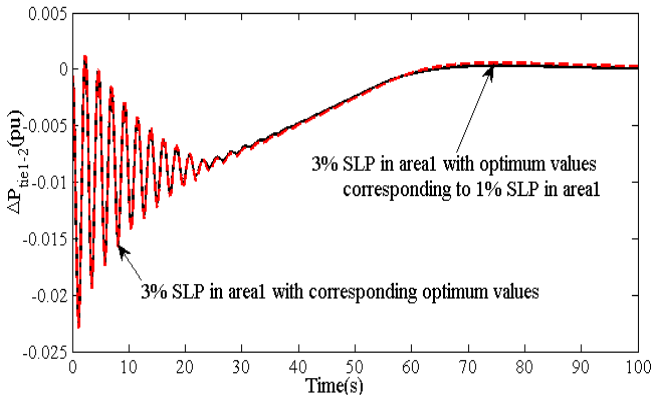

Fig. 13. ΔP_{tie1-2} vs. Time (s) at 3% SLP.

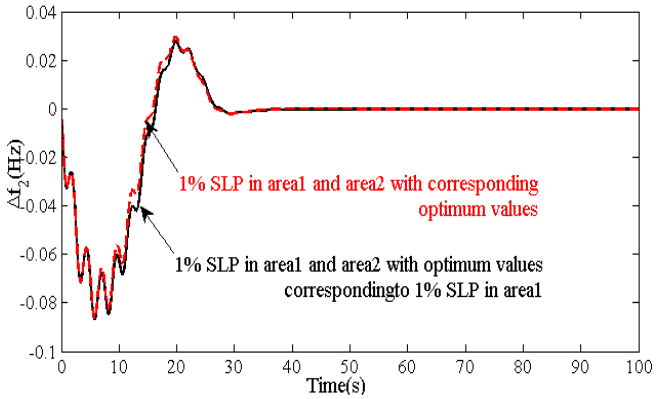

Fig. 14. Δf_2 vs. Time (s) at 1% SLP in areas-1 & 2.

5.2.4. The SA at varied location of perturbation

The nominal location of SLP is area1. This SLP location is changed to simultaneous occurrence in area-1, area-2 and area-1, area-2, area-3. In both the cases, the 2-DOF-PID controller gains (K_{Ii}, K_{Pi}, K_{Di}) and other parameters (b_i, c_i and N_i) are optimized separately using SOS technique and are mentioned in Table 4 (column 8 and column 9). At 1% in area-1, area-2 and simultaneous 1% SLP in area-1, area-2, area-3 the dynamic behaviors are plotted with optimum values corresponding for nominal position of SLP (area-1) and varied positions of SLP are presented in Fig.14 and Fig.15. From Fig.14 and Fig.15, it is observed that the responses (with nominal and varied position of SLPs) are nearly same. This demonstrates the toughness of 2-DOF-PID controller gains and additional parameters for variation in the locations of perturbation.

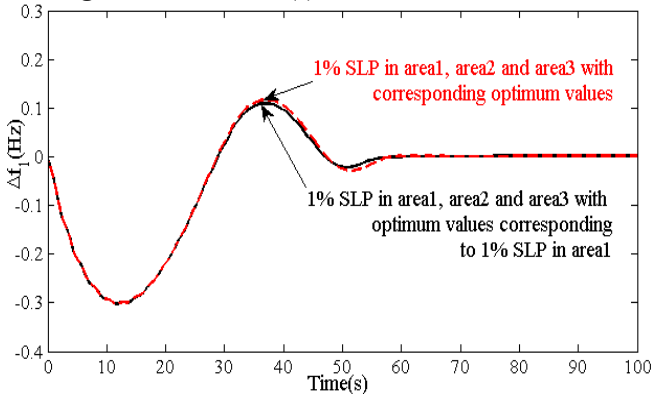

Fig. 15. Δf_1 vs. Time (s) at 1% SLP in all the three areas.

Table 4. Optimum parameters of 2-DOF-PID controller at altered circumstances.

Optimum parameter	Loading		Inertia constant		SLP magnitude		SLP position	
	-25%	+25%	-20%	+20%	2% in area-1	3% in area-1	1% in areas-1&2	1% in areas-1,2&3
K_{IDG}^*	0.0057	0.0123	0.0053	0.0091	0.0062	0.0077	0.1002	0.0055
K_{I1}^*	0.1606	0.1011	0.1002	0.0894	0.0932	0.1002	0.1002	0.1075
K_{I2}^*	0.1828	0.1553	0.3221	0.1222	0.1612	0.1702	0.2001	0.1533
K_{I3}^*	0.5413	0.6011	0.4924	0.4891	0.4709	0.4985	0.4961	0.4921
K_{PDG}^*	0.9717	0.9806	1.0000	0.9991	1.0000	0.9865	0.7955	0.9998
K_{P1}^*	0.4430	0.0341	0.0660	0.0806	0.0425	0.0511	0.0511	0.0319
K_{P2}^*	0.8440	0.8650	0.9685	0.9481	1.0000	0.9955	0.9963	0.8896
K_{P3}^*	0.9054	0.9723	1.0000	0.0943	0.9902	0.7963	1.0000	0.9026
K_{DDG}^*	0.9889	1.0000	0.9971	0.9993	1.0000	0.8963	1.0000	0.9898
K_{D1}^*	0.1996	0.3221	0.2963	0.3069	0.3203	0.2331	0.3120	0.1814
K_{D2}^*	0.4411	0.2943	0.2998	0.3183	0.3296	0.3221	0.2995	0.3221
K_{D3}^*	0.7251	0.8873	0.7383	0.7837	0.8525	0.7001	0.9121	0.8552
N_{DG}^*	10.000	10.000	10.000	10.036	10.000	19.635	21.032	21.702
N_1^*	37.208	70.059	66.052	78.383	98.987	80.112	79.613	74.678
N_2^*	38.139	33.529	17.083	35.055	40.632	40.221	41.123	33.346
N_3^*	72.257	88.144	72.380	88.426	79.357	79.526	89.363	80.412
b_{DG}^*	1.0000	1.0000	1.0000	1.000	0.9448	0.8552	1.000	1.000
b_1^*	0.4906	0.4863	0.6002	0.4999	0.4735	0.5521	0.6131	0.4265
b_2^*	0.9010	0.9988	0.5998	0.7963	0.8642	0.9110	1.000	0.9925
b_3^*	0.8497	0.7389	0.8304	0.9981	0.8494	0.8995	1.000	0.8326
c_{DG}^*	0.9999	0.9987	0.9933	1.0000	1.000	0.9663	0.9963	0.9805
c_1^*	0.3129	0.1963	0.1923	0.2399	0.3053	0.3001	0.3122	0.1805
c_2^*	1.0000	1.0000	1.0000	1.0000	0.9427	0.8874	0.9221	0.9174
c_3^*	0.2714	0.2951	0.5121	0.2191	0.2299	0.2661	0.2616	0.2253

Thus, from the responses, Fig.8 to Fig.15 it is concluded that the optimum parameters (gains and different parameters) of 2-DOF-PID controller attained at nominal circumstances are tough and not essential to retune for widespread deviations in the system circumstances like system loading, system inertia parameter (H) and magnitude, location of SLP.

5.3. The performance 2-DOF-PID controllers at varied (random) load pattern

In this case, the effectiveness of the 2-DOF-PID controller is evaluated when arbitrary or random load pattern (RLP) as shown in Fig.16 is applied. The RLP is applied separately in two ways, (1) as perturbation in Area1, and (2) as wind generator input (ΔP_{WTG}).

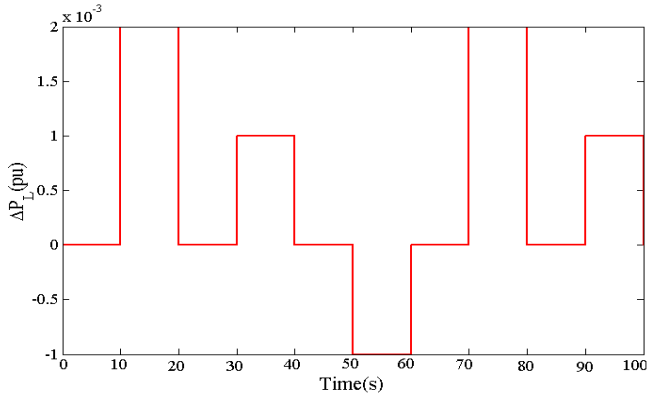

Fig. 16. The random load pattern (RLP).

When RLP applied as perturbation in area1, PID and 2-DOF-PID gains and different parameters are again optimized with SOS technique. The optimum gains and different parameters for PID and 2-DOF-PID controller are shown in Table 5. With optimum values mentioned in Table 5, the dynamics are plotted and compared for PID and 2-DOF-PID controllers in Fig.17. From Fig.17 it is seen that the 2-DOF-PID controller is providing better dynamics than PID controller with reduced oscillations.

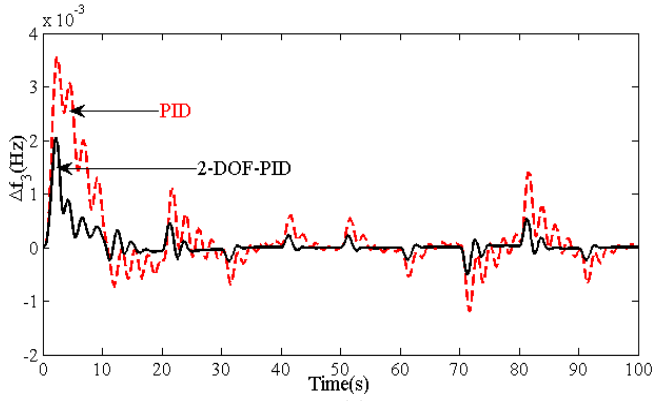

(a)

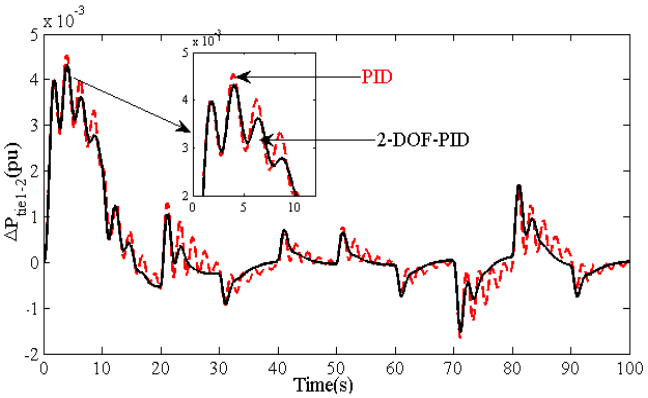

(b)

Fig. 17. The comparison performance for PID and 2-DOF-PID controllers at RLP.
(a) Δf_3 vs. Time (s)
(b) $\Delta P_{tie1\text{-}2}$ vs. Time (s).

Table 5. The PID and 2-DOF-PID controller optimum parameters with RLP as perturbation and wind turbine input.

Controller/ parameter	As perturbation		As wind turbine input	
	PID	2-DOF-PID	PID	2-DOF-PID
K_{IDG}^*	0.4110	1.0000	0.8596	0.9962
K_{I1}^*	0.4925	1.0000	1.0000	0.2520
K_{I2}^*	0.2966	0.0990	0.1733	0.4533
K_{I3}^*	0.0852	0.7020	0.9454	0.8977
K_{PDG}^*	0.1120	0.9970	0.2563	0.9994
K_{P1}^*	0.1022	0.5550	0.8220	0.1927
K_{P2}^*	0.1100	0.7940	0.1051	0.1632
K_{P3}^*	0.0185	0.6890	0.9454	0.9893
K_{DDG}^*	0.0021	1.0000	0.1452	0.9962
K_{D1}^*	0.0211	0.4520	0.4211	0.4000
K_{D2}^*	0.0023	0.0010	0.0004	0.3866
K_{D3}^*	0.0121	0.2650	0.01383	0.9599
N_{DG}^*	69.3250	10.000	37.4555	69.1230
N_1^*	59.6352	100.000	99.9985	93.5150
N_2^*	86.3252	42.5590	12.3781	100
N_3^*	68.6352	13.6950	66.4254	78.9010
b_{DG}^*	----	1.0000	----	0.8510
b_1^*	----	0.9710	----	0.9658
b_2^*	----	0.4520	----	0.9923
b_3^*	----	0.1330	----	1.0000
c_{DG}^*	----	1.0000	----	0.9912
c_1^*	----	0.2320	----	0.0747
c_2^*	----	0.3800	----	0.0232
c_3^*	----	0.0010	----	0.2363

Similarly RLP is applied as random input for wind turbine (ΔP_{WTG}). Here also, the gains and different parameters of PID and 2-DOF-PID controllers are again optimized and are shown in Table 5. With these optimum values, the responses between PID and 2-DOF-PID controllers are compared in Fig.18. From Fig.18, it is realized that 2-DOF-PID controller performs better when compared with PID controller in providing the reduced oscillations.

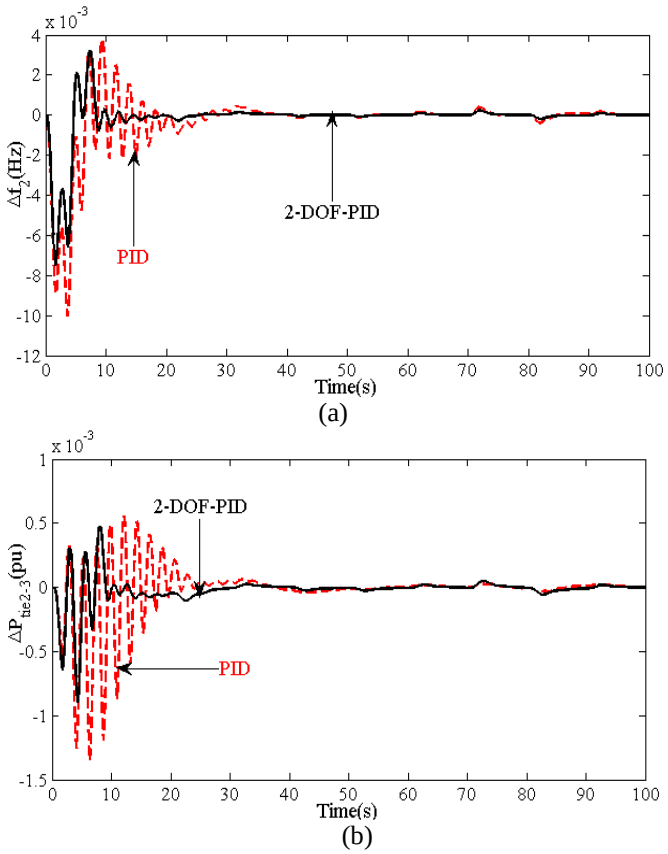

Fig. 18. Comparison performance of PID and 2-DOF-PID at RLP as wind turbine input.
(a) Δf_2 vs. Time (s).
(b) $\Delta P_{tie2\text{-}3}$ vs. Time (s).

6. Conclusion

Distributed generation (DG) resources such as wind turbine generators, fuel cells, diesel engine generators, aqua-electrolyzer, and battery energy storage system are incorporated into unequal three-area thermal system. The powerful metaheuristic symbiotic organisms search (SOS) technique is applied for optimizing the gains and different parameters of secondary controllers namely 2-DOF-PID, PID, PI and I controllers. The SOS optimized 2-DOF-PID controller provides superior performance than others in terms of reduced peak overshoots, minimum settling time and lesser cost value. The SOS techniques outperforms particle swarm optimization and firefly algorithms. Sensitivity analysis is evident for the toughness of gains and different parameters of 2-DOF-PID controller found at nominal circumstances for large deviations in system loading condition, inertia parameter and magnitude, location of perturbation. The 2-DOF-PID controller performance is found satisfactory in the event of RLP at perturbation as well as wind turbine input.

Appendix

frequency (f) = 60 Hz; i, * are subscript and superscript to denote area i and optimum value; inertia constant (H) = 5 s; governor time constant (T_{gi}) = 0.08 s; turbine time constant (T_{ti}) = 0.3 s; reheat time constant (T_{ri}) = 10 s; reheat gain (K_{ri}) = 0.5; gain of power system (K_{pi}) = $1/D_i$ = 120 Hz/pu MW; power system time constant (T_{pi}) = $2.H_i$ / $f.D_i$ = 20 s; synchronizing power coefficient (T_{ij}) = 0.086 pu MW/rad; ΔP_{Di} is load change; $D_i = \Delta P_{Di} / \Delta f_i$ (pu/Hz) = 8.33×10^{-3} pu MW/Hz; frequency bias (B_i) = area frequency response characteristic (- β_i) = 0.425 pu MW/Hz; speed governor regulation parameter (R_i) = 2.4 pu Hz/MW; loading = 50%, wind turbine time constant (T_{WTG}) = 1.5 s; gain of wind turbine (K_{WTG}) = 1; gain of aqua-electrolyzer (K_{AE}) = 0.002; aqua-electrolyzer time constant (T_{AE}) = 0.5 s; gain of fuel cell (K_{FC}) = 0.01; time constant of fuel cell (T_{FC}) = 4 s; gain of diesel engine generator (K_{DEG}) = 0.0003; time constant of diesel engine generator (T_{DEG}) = 2.0 s; gain of battery energy storage system (K_{BESS}) = - 0.0003) time constant of battery energy storage system (T_{BESS}) = 0.1 s; Δf_i, ΔP_{tie} are deviations in frequency and tie-line powers; pi = π; T is the simulation time; K_{Pi}, K_{Ii}, K_{Di} are the proportional, integral and derivative gains of SCs; N_i is the filter coefficient; b_i and c_i are the integral and derivative set-point weights of 2-DOF-PID controller.

References

[1] O. I. Elgerd and C. E. Fosha, "Optimum Megawatt-Frequency Control of Multiarea Electric Energy Systems", IEEE Transactions on Power Apparatus and Systems, Vol. PAS-89, No. 4, pp. 556-563, April 1970.

[2] K. D. Mercado, J. Jiménez and M. C. G. Quintero, "Hybrid renewable energy system based on intelligent optimization techniques", IEEE International Conference on Renewable Energy Research and Applications (ICRERA), Birmingham, pp. 661-666, 20-23 November 2016.

[3] E. Kabalci, R. Bayindir and E. Hossain, "Hybrid microgrid testbed involving wind/solar/fuel cell plants: A desing and analysis testbed", International Conference on Renewable Energy Research and Application (ICRERA), Milwaukee, WI, , pp. 880-885, October 2014.

[4] S. Belgana, A. Dabib, H. Bilil and M. Maaroufi, "Hybrid renewable energy system design using multobjective optimization", International Conference on Renewable Energy Research and Applications (ICRERA), Madrid, pp. 955-960, October 2013.

[5] R. Ali, Y. S. Qudaih, Y. Mitani and T. H. Mohamed, "A robust load frequency control of power system with fluctuation of renewable energy sources", International Conference on Renewable Energy Research and Applications (ICRERA), Madrid, pp. 711-716, October 2013.

[6] N. S. Jayalakshmi, D. N. Gaonkar and P. B. Nempu, "Power Control of PV/Fuel Cell/Supercapacitor Hybrid System for Stand-Alone Applications", International Journal of Renewable Energy Research, Vol.6, No.2, pp. 672-679, 2016.

[7] I. Hussain, S. Ranjan, D. C. Das and N. Sinha, "Performance Analysis of Flower Pollination Algorithm Optimized PID Controller for Wind-PV-SMES-BESS-

Diesel Autonomous Hybrid Power System", International Journal of Renewable Energy Research, Vol.7, No.2, pp. 643-651, 2017.

[8] A. J. Veronica and N. S. Kumar, "Load Frequency Controller Design for Microgrid using Internal Model Control Approach", International Journal of Renewable Energy Research, Vol.7, No.2, pp. 778-786, 2017.

[9] S. M. Vaca, C. Patsios and P. Taylor, "Enhancing frequency response of wind farms using hybrid energy storage systems", IEEE International Conference on Renewable Energy Research and Applications (ICRERA), Birmingham, pp. 325-329, November 2016.

[10] L. Hui, L. Shengquan, J. Haiting, Y. Dong, Y. Chao, C. Hongwen, Z. Bin, H. Yaogang and C. Zhe, "Damping control strategies of inter-area low-frequency oscillation for DFIG-based wind farms integrated into a power system", Int. J. Electr. Power Energy Syst., Vol. 61, pp. 279-287, 2014.

[11] V. P. Singh, S. R. Mohanty, N. Kishor and P. K. Ray, "Robust H-infinity load frequency control in hybrid distributed generation system", Int. J. Electr. Power Energy Syst., Vol. 46, pp. 294-305, 2013.

[12] P. K. Ray, S. R. Mohanty and N. Kishor, "Proportional–integral controller based small-signal analysis of hybrid distributed generation systems", Int. J. Energy of conversion Management, Vol. 52, No. 4, 1943-1954, 2011.

[13] R. K. Sahu, S. Panda and U. K. Rout, "DE optimized parallel 2-DOF PID controller for load frequency control of power system with governor dead-band nonlinearity", Int. J. Electr. Power Energy Syst., Vol. 49, pp. 19–33, 2013.

[14] N. Pathak, T.S. Bhatti and A. Verma, "New performance indices for the optimization of controller gains of automatic generation control of an interconnected thermal power system", Sustainable Energy, Grids and Networks, Vol. 9, pp. 27-37, 2017.

[15] H. Gozde, and M. C. Taplamacio, "Automatic generation control application with craziness based particle swarm optimization in a thermal power system", Int. J. Electr. Power Energy Syst., Vol. 33, No. 1, pp. 8-16, 2011.

[16] M. Elsisi, M. Soliman, M. A. S. Aboelela and W. Mansour, "Bat inspired algorithm based optimal design of model predictive load frequency control", Int. J. Electr. Power Energy Syst., Vol. 83, pp. 426-433, 2016.

[17] M. Raju, L. C. Saikia and N. Sinha, "Automatic generation control of a multi-area system using ant lion optimizer algorithm based PID plus second order derivative controller", Int. J. Electr. Power Energy Syst., Vol. 80, pp. 52-63, 2016.

[18] R. K. Sahu, S. Panda, A. Biswal and G. T. C. Sekhar, "Design and analysis of tilt integral derivative controller with filter for load frequency control of multi-area interconnected power systems", ISA Transactions, Vol. 61, pp. 251-264, 2016.

[19] L. C. Saikia, N. Sinha and J. Nanda "Maiden application bacterial foraging based fuzzy IDD controller in AGC of a multi-area hydrothermal system", Int. J. Electr. Power Energy Syst., Vol. 45, No. 1, pp. 98-106, 2013.

[20] L. C. Saikia, S. Mishra, N. Sinha and J. Nanda, "Automatic generation control of a multi area hydrothermal system using reinforced learning neural network controller", Int. J. Electr. Power Energy Syst., Vol. 33, No. 4, pp. 1101-1108, 2011.

[21] S. K. Pandey, S. R. Mohanty, N. Kishor and J. P. S. Catalão, "Frequency regulation in hybrid power systems using particle swarm optimization and linear matrix inequalities based robust controller design", Int. J. Electr. Power Energy Syst., Vol. 63, pp. 887-900, 2014.

[22] J. Nanda, A. Mangla, and S. Suri, "Some New Findings on Automatic Generation Control of an Interconnected Hydrothermal System with Conventional Controllers", IEEE Transactions on Energy Conversion, Vol. 21, No. 1, pp. 187-194, 2006.

[23] S. Panda and N. K. Yegireddy, "Automatic generation control of multi-area power system using multi-objective non-dominated sorting genetic algorithm-II", Int. J. Electr. Power Energy Syst., Vol. 53, pp. 54-63, 2013.

[24] E. S. Ali and S. M. Abd-Elazim, "BFOA based design of PID controller for two area Load Frequency Control with nonlinearities", Int. J. Electr. Power Energy Syst., Vol. 51, pp. 224-231, 2013.

[25] L. C. Saikia, J. Nanda and S. Mishra, "Performance comparison of several classical controllers in AGC for multi-area interconnected thermal system", Int J. Electr. Power Energy Syst., Vol. 33, No. 3, pp. 394-401, 2011.

[26] R. K. Sahu, S. Panda, U. K. Rout and D. K. Sahoo, "Teaching learning based optimization algorithm for automatic generation control of power system using 2-DOF PID controller, Int J. Electr. Power Energy Syst., Vol. 77, pp. 287-301, 2016.

[27] V. Soni, G. Parmar, M. Kumar and S. Panda, "hGWO-PS Optimized 2DOF-PID Controller for Non Reheat Two Areas Interconnected Thermal Power Plants: A Comparative Study", IEEE 1st International Conference on Power Electronics, Intelligent Control and Energy Systems (ICPEICES), pp. 1-6, 2016.

[28] P. Dash, L. C. Saikia and N. Sinha, "Comparison of performances of several Cuckoo search algorithm based 2DOF controllers in AGC of multi-area thermal system", Int. J. Electr. Power Energy Syst., Vol. 55, 429-436, 2014.

[29] K. Yamashita and T. Taniguchi, "Optimal observer design for load frequency control", Int. J. Electr. Power Energy Syst., Vol. 8, No. 2, pp. 93-100, 1986.

[30] S. P. Ghoshal and S. K. Goswami, "Application of GA based optimal integral gains in fuzzy based active power-frequency control of non-reheat and reheat thermal generating systems", Electric Power Systems Research, Vol. 67, No. 2, pp. 79-88, 2003.

[31] H. Gozde, M. C. Taplamacioglu and I. Kocaarslan, "Comparative performance analysis of Artificial Bee Colony algorithm in automatic generation control for interconnected reheat thermal power system", Int. J. Electr. Power Energy Syst., Vol. 42, No. 1, pp. 167-178, 2012.

[32] S. Debbarma, L. C. Saikia and N. Sinha, "Solution to automatic generation control problem using firefly algorithm optimized $I^{\lambda}D^{\mu}$ controller", ISA Transactions, Vol. 53, No. 2, pp. 358-366, 2014.

[33] M. Cheng and D. Prayogo, "Symbiotic Organisms Search: A new metaheuristic optimization algorithm", International Journal of Computers and Structures, Vol. 139, pp. 98-112, 2014.

[34] P. Dash, L. C. Saikia and N. Sinha, "Automatic generation control of multi area thermal system using Bat algorithm optimized PD–PID cascade controller", Int. J. Electr. Power Energy Syst., Vol. 68, pp. 364-372. 2015.

[35] D. J. Lee and L. Wang, "Small-Signal Stability Analysis of an Autonomous Hybrid Renewable Energy Power Generation/Energy Storage System Part I: Time-Domain Simulations", IEEE Transactions on Energy Conversion, Vol. 23, No. 1, pp. 311-320, 2008.

[36] M. Araki and H. Taguchi, "Two-degree-of-freedom PID controllers", International Journal of Control, Automation and Systems, Vol. 1, No. 4, pp. 401-411, 2003.

[37] J. Sanchez, A. Visioli and S. Dormido, "A two-degree-of-freedom PI controller based on events", Journal of Process Control, Vol. 21, No. 4, pp. 639-651, 2011.

[38] Y. M. Zhao, W. F. Xie and X. W. Tu, "Performance-based parameter tuning method of model-driven PID control systems", ISA Transactions, Vol. 51, No. 3, pp. 393-399, 2012.